Filtering and Detection of Low Contrast Structures on Ultrasound Images

Lorena Vargas-Quintero[a], Boris Escalante-Ramírez[a], Fernando Arámbula[b]
[a]Dep. de Procesamiento de Señales, Facultad de Ingeniería; [b]Centro de Ciencias Aplicadas y Desarrollo Tecnológico
Universidad Nacional Autónoma de México

ABSTRACT

In this paper, we propose a detection method of low contrast structures in medical ultrasound images. Since noise speckle makes difficult the analysis of ultrasound images, two approaches based on the wavelet and Hermite-transforms for enhancement and noise reduction are compared. These techniques assume that speckle pattern is a random signal characterized by a Rayleigh distribution and affects the image as a multiplicative noise. For the wavelet-based approach, a Bayesian estimator at subband level for pixel classification is used. All the estimation parameters are calculated using an adjustment method derived from the first and second order statistical moments. The Hermite method computes a mask to find those pixels that are corrupted by speckle. In this work, we consider a statistical detection model that depends on the variable size and contrast of the image speckle. The algorithms have been evaluated using several real and synthetic ultrasound images. Combinations of the implemented methods can be helpful for automatic detection applications of tumors in mammographic ultrasound images. The employed filtering techniques are quantitatively and qualitatively compared with other previously published methods applied on ultrasound medical images.

Keywords: Speckle, Hermite Transform, Wavelet Transform, Ultrasound image, Detection Theory.

1. INTRODUCTION

Ultrasound is a medical imaging modality that is widely used in clinical applications. It is based on the transmission of high frequency sound waves into the body. The returning pulse-echoes are captured and processed to build the digital image. Unfortunately, these images are often characterized by low contrast and intrinsic artifacts called speckle, which is the result of constructive and destructive coherent interferences of the back scattered ultrasound echoes.

Lesion detection tasks, such as small cancerous lesions and cysts, using ultrasound images are very common. Currently, there are several techniques that allow solving this problem but many of them differ in efficiency, speed and process optimization. High performance is searched in the detection process since it may seriously affect the medical diagnosis. For this reason, in ultrasound image it is very important consider some characteristics such as spatial and contrast resolutions as well as noise have to be considered.

Several methods have been developed to assist ultrasound diagnosis, which allow physicians to find information present in the images that is not easily detected. Examples are found in the development of techniques devoted to the automatic measurement of fetal organs or gynecological problems[1]. However, the limited contrast of ultrasound images can cause some problems in the differentiation of soft tissue or lesions[2].

Barrett et al. based their results on objective assessment of image quality and ideal observer performance for detection tasks[3]. Their work offers a rigorous treatment of ideal observers, and proposes some suitable analytical techniques for performance assessment.

In the literature, there are several ultrasound imaging statistical models[4]. Smith and Wagner[5 -7], e.g., take from Goodman[8] the speckle statistic models for ultrasound images. Detection performance, as studied by Wagner[5 -7], assumes linear shift-invariance, large area lesions, low contrast lesions and independent samples. In the same way, they analyzed the ultrasound B-mode images from a stochastic theory point of view.

Optics, Photonics, and Digital Technologies for Multimedia Applications II, edited by
Peter Schelkens, Touradj Ebrahimi, Gabriel Cristóbal, Frédéric Truchetet, Pasi Saarikko,
Proc. of SPIE Vol. 8436, 84361F · © 2012 SPIE · CCC code: 0277-786X/12/$18 · doi: 10.1117/12.922861

Insana and Hall[9] interpreted the developments made by Smith and Wagner theories. They conducted experiments to measure how close humans are at low-contrast lesion detection in B-mode images from the ideal observer performance. Clarkson and Barrett[10] discuss the ideal observer for a number of different detection tasks and probability models.

On the other hand, its noninvasive nature, the speed, low cost and the portability of scanners, make ultrasound imaging an attractive tool for medical diagnosis. However, it presents some limitations including image quality and speckle pattern effects which hinder visual interpretation.

For the solution of these problems, several filtering techniques have been proposed with the aim of enhancing ultrasound images. Most speckle filters are developed for enhancing visualization of speckle images in spatial domain[11]. Yu and Acton[12] developed the Speckle Reducing Anisotropic Diffusion (SRAD) by showing that Lee[26] filters can be represented as partial differential equations. Then, SRAD is derived by allowing an edge-sensitive anisotropic diffusion within this context. Loizou[11] et al., implemented a solution for SRAD based on filters and local statistics.

Recently, several attempts have been made to reduce the speckle noise using wavelet transforms as a multi-resolution image processing tool. Techniques based on wavelets can be classified into two categories: homomorphic filtering and non homomorphic filtering. The first process is applied on a logarithmic transformation and it is followed by an exponential transformation[13, 22]. The process for the non homomorphic is realized onto the original image and the most notable approaches are proposed by Pizurica[14]. Moreover, Yue[15] et al. developed a novel Multiscale Nonlinear Wavelet Diffusion method for ultrasound speckle suppression and edge enhancement.

In this paper, we compare findings obtained for Hermite-based method proposed by Escalante-Ramirez[16 -18] et al., with the wavelet-based Bayesian approach developed by Gupta[22] et al. We adopted these techniques because they have demonstrated being efficient to remove speckle patterns while the edges are preserved.

The main objective of this work is to make an implementation of filtering and detection algorithms for applications of low contrast structures in ultrasound images. We compared the performance of the detection methods when a filtering process for speckle suppression is previously applied.

The rest of the paper is organized as follows. Section 2 presents a general description of the implemented system. In section 3, two statistical detection models are shown. Model of the speckle image and filtering techniques adopted in this paper are analyzed in section 4. Speckle reduction results obtained using different filters and detection performance results are described in section 5. Finally, conclusions and future works are presented in section 6.

2. SYSTEM DESCRIPTION

Figure 1 describes a general block diagram of the steps followed in this work. We focus our work in evaluating decision theories with ultrasound images for lesion detection applications. The analysis is made using original images and their filtered versions. We assume that lesions in the ultrasound images are coded as areas of increasing variance. From a visual point of view, our ultrasound images are characterized by a bright structure surrounded by a dark background when lesions are present.

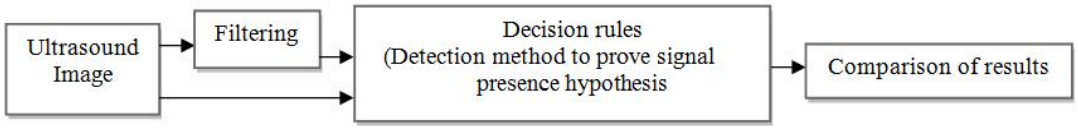

Figure 1. Block diagram of the general system.

Likewise, we try to verify how much the filtering process influences the detection when automatic algorithms are used. As described, several filtering algorithms are employed. Two decisions rules are evaluated with filtered and non- filtered real and synthetic images.

3. DETECTION THEORY

In the detection analysis of a B-mode scans, the statistical properties of the image must be considered. The speckle pattern is due to interference of sound wavelets scattered by structures or tissue. In this paper, the speckle pattern is analyzed using stochastic signal theory such as Goodman[8], Smith and Wagner[5, 7] exposed in their works. Formulations for speckle modeling in ultrasound B-Scan images adopt the coherent optical theory for laser systems.

Lesion detectability in this type of images is deduced from the first and second order statistical moments of the speckle. We study two cases for the ultrasound images: 1) Firstly, we assume that each ultrasound image is a realization of a stochastic process that exhibits a Rayleigh distribution; 2) Secondly, images possess Gaussian distributions as a result of the summation of multiple random processes in the ultrasound system. In this process, the sample images are considered as vectors or signals denoted by $\boldsymbol{x}$. which is carried out by the concatenation of each column.

The detection technique is based on a binary decision rule in which one of two possibilities is selected. For the case of lesion detection in ultrasound images, the algorithm must decide if the abnormality is present or not. Because speckle is present in the image in both cases, we must define a conditional probability density functions when the lesion is present and when it is absent.

3.1 Rayleigh distribution case

A Rayleigh distribution[8] for the ultrasound image magnitude appears when the signals that form each point of the image are complex Gaussian random fields that result from the addition of real and imaginary components (a_r and a_i). For the statistical model, it is assumed that the random variables that compose the random field are not correlated and independent. The probability density function for the signal present and absent can be written, respectively as:

$$f(x_i/\psi_1)=\prod_{i=0}^{M}\frac{x_i}{\psi_1^2}\exp\left(-\frac{x_i^2}{2\psi_1^2}\right) \quad , \quad f(x_i/\psi_2)=\prod_{i=0}^{M}\frac{x_i}{\psi_2^2}\exp\left(-\frac{x_i^2}{2\psi_2^2}\right) \tag{1}$$

where $f(x_i/\psi_1)$ is the probability density function for the signal present and $f(x_i/\psi_2)$ is the probability density function for the signal absent.

Using Bayes theory, the likelihood ratio for the signals is calculated[5-7]:

$$\frac{f(x_i/\psi_1)}{f(x_i/\psi_2)}=\prod_{i=1}^{M}\frac{\psi_1}{\psi_2}\exp\left(-\frac{x_i^2}{2}\left(\frac{1}{\psi_2}-\frac{1}{\psi_1}\right)\right) \tag{2}$$

Applying logarithm transformation and knowing that the factors ψ are constant[7], the equation for the decision function is finally obtained:

$$\gamma=\sum_{i=1}^{M}x_i^2 \qquad 1\le i\le M \tag{3}$$

The final decision rule is applied by comparing γ with a threshold. M represents the number of pixels analyzed. Instead of measuring the speckle spot area, as suggested by Smith[7], we measure the pixels of the whole image because we consider that each ultrasound image is a stochastic process with no certainty of the presence of a lesion.

3.2 Gaussian distribution case

In the second case, a Gaussian distribution assumes that the image is a contribution from many random processes in the ultrasound system. According to the central limit theorem, for large values of M a Gaussian distribution is obtained. The joint density function for N random variables is computed as:

$$f(\vec{x}/K_s)=\frac{\left(\left(K_s\right)^{-1}\right)^{-1/2}}{\left(2\pi\right)^{N/2}}\exp\left[-\frac{\left(\vec{x}-\vec{x}\right)^T K_s^{-1}\left(\vec{x}-\vec{x}\right)}{2}\right] \tag{4}$$

where x is the vector that contains the random variables; K_s is the covariance matrix (s = 0, 1) for the signal present and absent which correlates the random variables that compose the image. The log likelihood ratio is the decision function. For the Gaussian case, the decision rule[29] is calculated as:

$$\gamma = x^t \left(K_0^{-1} - K_1^{-1} \right) x \tag{5}$$

where K_0 and K_1 are the covariance matrices for the absent and present signals, respectively. As in the previous case, the decision rule depends on a threshold that determines if a lesion is present or not.

4. FILTERING METHODS FOR ULTRASOUND IMAGES

Speckle in ultrasound B-scans is seen as a granular structure which is caused by the constructive and destructive coherent interferences of back scattered echoes from the scatters that are typically much smaller than the spatial resolution of medical ultrasound system. This phenomenon is common to laser, sonar and synthetic aperture radar imagery (SAR). Speckle pattern is a form of multiplicative noise and it depends on the structure of image tissue and various imaging parameters[32]. Having a general speckle model is important for formulating techniques that reduce these patterns in ultrasound images. There are many formulations[13, 14] that agree in modeling speckle images as:

$$g(i,j) = y(i,j) \cdot n(i,j) \tag{6}$$

where y is the noise free image, n is an arbitrary speckle pattern contribution and g corresponds to the noisy observation; *(i, j)* are the spatial coordinates in the image. The additive noise component is insignificant with respect to the multiplicative component. For this reason, it is not considered in the last equation. The multiplicative components are transformed into additive by applying a logarithmic transformation,

$$\log(g(i,j)) = \log(y(i,j)) + \log(n(i,j)) \tag{7}$$

Thus, the signal model of equation (6) can be written as:

$$p(i,j) = x(i,j) + N(i,j) \tag{8}$$

Now, additive noise suppression methods can be applied to equation (8) for the speckle reduction. Once the filtering process is carried out, the image is returned to original space by computing an exponential transformation.

In this paper, we analyze different filtering techniques for ultrasound images. We show results for several approaches for speckle reduction: 1) Algorithm proposed by Donoho[20] which consists of a soft-thresholding method using wavelet decomposition; 2) Lee approach[26] that uses a statistical technique to define a noise model in order to subsequently apply a local statistical filter; 3) Wiener filter[19, 33] which estimates the local variance and mean around each pixel to develop a local and adaptive estimation using the found parameters and 4) Pizurica's method[14] consisting of a wavelet-based algorithm that exploits the correlation of significant image features across the resolution scales to perform a preliminary coefficient classification. This is afterwards used to empirically estimate the statistical distributions of the coefficients that represent significant image features on the one hand and mainly noise on the other. Technical and implementation details can be reviewed in the cited references.

Other considered filters are based on the Hermite transform[16-18], proposed by Escalante-Ramirez et al., and wavelet Bayesian theory[22] developed by Gupta[22].

Generally speaking, Hermite and wavelet approaches use multiresolution representations for the filtering process. In figure 2 a general diagram of the filtering sequence used for these two techniques is shown.

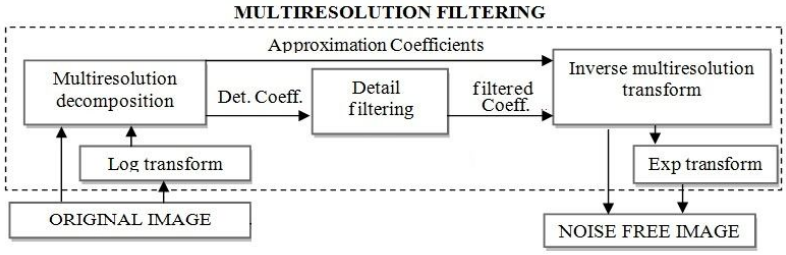

Figure 2. General scheme of the filtering system using multiresolution analysis for Hermite and wavelet approaches.

The process in the last scheme starts by changing the domain of the input image and continues filtering the resulting coefficients. Finally, the filtered resulting image is calculated by returning to the original representation space. Some details of these techniques are described below. In the case of the wavelet-based approach, a logarithmic transformation is firstly applied before making the multiresolution decomposition. In contrast, Hermite-based approach decomposes the original image without previous transformation.

4.1 Wavelet filtering

Wavelet decomposition produces a family of hierarchically organized decompositions, i.e., a signal is decomposed into a hierarchical set of approximations and details. A wavelet prototype function, called an analyzing wavelet or mother wavelet[23] is selected to analyze the image.

The two-dimensional Discrete Wavelet Transform is defined mathematically as:

$$C(a,b) = C(j,k) = \sum_{x \in Z} \sum_{y \in Z} f(x,y) g_{j,k}(x,y) \tag{9}$$

where $a = 2^j, \quad b = k2^j, \quad j \in N, \; j \in N$

f is the original image, *g* is the wavelet function, *a* is a scale factor of the wavelet function, *b* is a position parameter and *C(a,b)* is the set of transform coefficients.

In general, when the wavelet transform is used for filtering, each subband is modified using some criteria depending on the characteristics of the images. In the case of ultrasound images, the process is applied on the detail coefficients which represent the high frequency information.

Once the subbands are filtered, the resulting image is obtained by applying the inverse process calculated by:

$$f(x,y) = \sum_{j \in Z} \sum_{k \in Z} C(j,k) \psi_{j,k}(x,y) \tag{10}$$

where ψ is the wavelet function. Barba[24, 34] et al., provide a complete explication of this process.

4.1.1 Wavelet-based Bayesian approach

Gupta[13, 22] et al., proposed a method in which a Rayleigh distribution is used for modeling speckle noise and a Gaussian distribution for the original ultrasound image. Therefore, the probability density function (pdf) of the Rayleigh distribution[28] that characterized the speckle noise can be defined by the equation:

$$p = \frac{n}{\alpha^2} \exp\left(-\frac{n^2}{2\alpha^2} \right) \qquad n \geq 0 \tag{11}$$

Mihck[25] et al., demonstrated that the histogram of the wavelet coefficients can be approximated by the zero mean Gaussian distribution. Mathematically, this can be represented as:

$$p = \frac{1}{\sigma\sqrt{2\pi}} \exp\left(-\frac{x^2}{2\sigma^2} \right) \qquad -\infty < x < \infty \tag{12}$$

Therefore, using these equations, and according to the MAP theory and the Bayes rules, Gupta[13, 22] et al., found a final estimation expression to enhance each subband of the wavelet transform:

$$\hat{x}(y) = sign(y) \cdot \left(\max\left(0, \frac{\left(2|y|\sigma_x^2 + \alpha^2 |y| - \sqrt{\alpha^4 y^2 + 4\alpha^2 \sigma_x^2 + 4\alpha^2 \sigma_x^4} \right)}{2(\alpha^2 + \sigma_x^2)} \right) \right) \tag{13}$$

where $\alpha = \sigma / \sqrt{2}$; σ^2 is the noise variance, it is estimated by $\hat{\sigma}^2 = C\left[\frac{median|y|}{0.6745} \right]$; y corresponds to the first and second level diagonal detail subbands; C is a constant that control the noise level to be eliminated. Finally, $\hat{\sigma}_x = \sqrt{\max(\hat{\sigma}_y^2 - \hat{\sigma}^2, 0)}$ is the standard deviation of the signal and $\hat{\sigma}_y^2$ is the wavelet coefficient variance.

4.2 Hermite transform for image filtering

The Hermite transform is a special case of polynomial transforms that can be used for multirresolution image analysis as well. The polynomial transform allows obtaining an image decomposition localized by a window function. Several window sizes are used in order to obtain a multiresolution analysis. Image polynomial coefficients $L_{m,n-m}(p,q)$ are obtained by the convolution of the original image $L(x,y)$ with the analysis filters::

$$D_{m,n-m}(x,y) = G_{m,n-m}(-x,-y)\ V^2(-x,-y). \tag{14}$$

The inverse polynomial transform is computed by interpolation

$$\hat{L}(x,y) = \sum_{n=0}^{N} \sum_{m=0}^{n} \sum_{(p,q)\in S} L_{m,n-m}(p,q) P_{m,m-n}(x-p, y-q) \tag{15}$$

where $L_{m,n-m}(p,q)$ are the polynomial coefficients; $P_{m,m-n}(x-p, y-q) = G_{m,n-m}(x,y)V(x,y)/W(x,y)$ are the interpolation function whose weighting function can be calculated through $W(x,y) = \sum_{(p,q)\in S} V(x-p, y-q)$,

$V(x,y)$ is the localization function window function that, in the case of the Hermite transform, corresponds to a Gaussian function. In this case, the set of orthogonal polynomials corresponds to the Hermite polynomials [16-18].

The process of filtering using the Hermite transform is similar to wavelet-based methods. The idea is to change the space of representation and then apply the corresponding filters. In order to return to the original space, the inverse process must be calculated.

4.2.1 Speckle noise reduction algorithm using polynomial transform

In this algorithm an energy mask is estimated which indicates the location of edges on the image. The mask is calculated from the first order energy image which corresponds to the first order coefficients of the Hermite transform. The estimated mask allows detecting edge positions of the image even if they are corrupted by speckle noise. The pixels corresponding to noisy homogeneous areas are then suppressed while image edges are enhanced.

The first order energy image corresponding to the convolution of the input image L with the first order derivatives of a Gaussian function can be used to separate edges from noise using thresholding techniques. The threshold can be found by:

$$T(x,y) = \frac{2\alpha \ln\left(\frac{1}{P_R} \right) L_{00}^2}{AN} \tag{16}$$

where $\alpha = |R_L(x,y) * D_{10}(x,y) * D_{01}(x,y)|_{x=y=0}$ and R_L is the auto-correlation function of L; P_R is the percentage of noise allowed to remain in the image; L_{00} is the zero order coefficient and A is the SNR^2_{llook}, $\sigma_l = \mu_l / (\sqrt{N} SNR_{lloop})$; N is the number of looks of L. This algorithm can be reviewed with more detail in Escalante-Ramirez[17] et al.

5. RESULTS AND DISCUSSIONS

We start our study by using three types of test images. 1) Synthetic ultrasound images which can be simulated as the magnitude of a complex Gaussian random field that has been lowpass-filtered[14]. For this task, we built and algorithm that is capable of generating synthetic ultrasound images. 2) Public simulated images using FIELD II, a free domain ultrasound simulator[31]. 3) Real speckled ultrasound images. In total, 148 images of size 120 x 120 pixels are used for validation. Quantitative and qualitative analysis was carried out for the filtering and detection algorithms.

5.1 Filtering results

We present in figure 3 visual results of the filtering process for several filters applied onto a simulated ultrasound image. This image was obtained from[14] and corresponds to a common sample used in the literature for algorithms validation. These filters are: Wiener filter[30], soft thresholding[20], wavelet-based Bayesian method[13, 22] and Hermite-based approach[17].

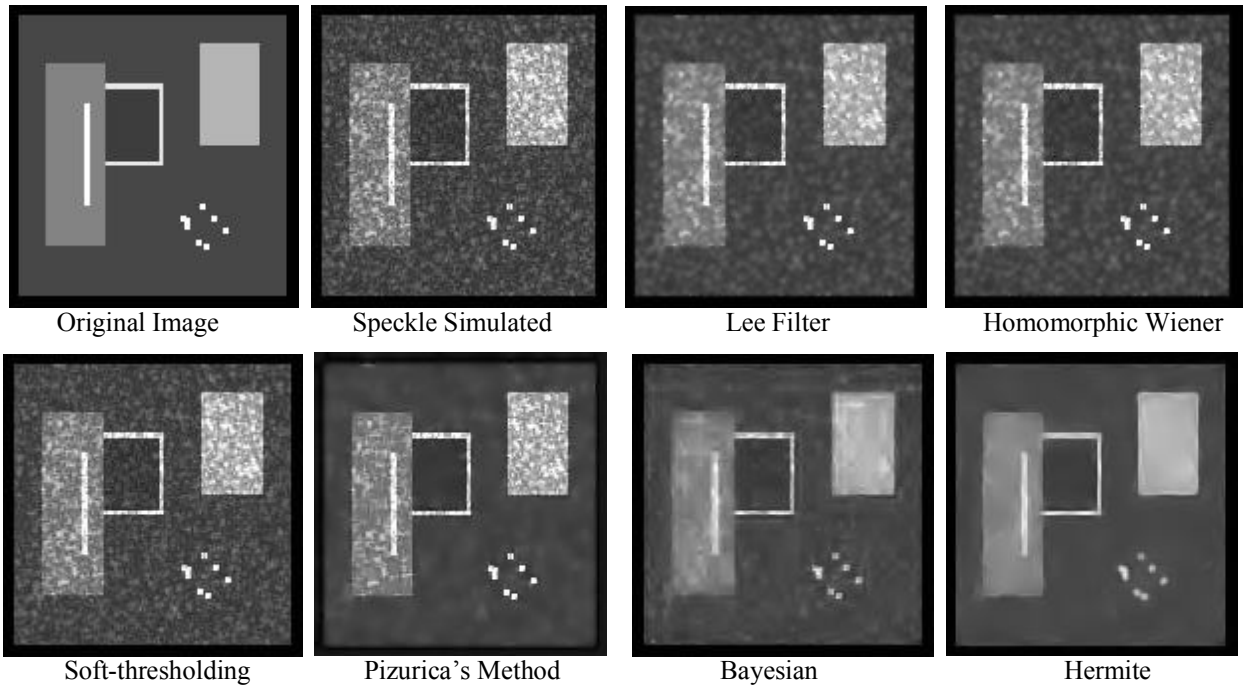

Figure 3. Visual comparison of several reduction speckle filtering on a 150 x 150 simulated speckle image (SNR = 4.28 dB)

Because the goal of this paper is to compare the above mentioned methods in the process of lesion detection, we used a simulated image (see figure 4) which presents a common low contrast structure that can be considered as a lesion in real ultrasound studies. The image was generated using FIELD II software[31].

From the visual results illustrated in figures 3, 4 and 5, it is noticed that a better performance is obtained with the Hermite-based approach. This filter appears to be much more efficient than the rest in removing speckle patterns while the edges of the images are preserved. Lee and Wiener filters get to preserve the edges, but they are poor in reducing speckle in homogeneous areas. Soft-thresholding demonstrates to have a deficient performance in the task of speckle reduction. The resulting filtered image is very similar to the original one.

Pizurica's method aims at preserving the edges of the images but the speckle pattern is still present to human observers. The wavelet-based Bayesian is a method that proves to be efficient to reduce speckle pattern but image edges are considerably blurred. Hermite technique reduces speckle while preserving the edges of the image.

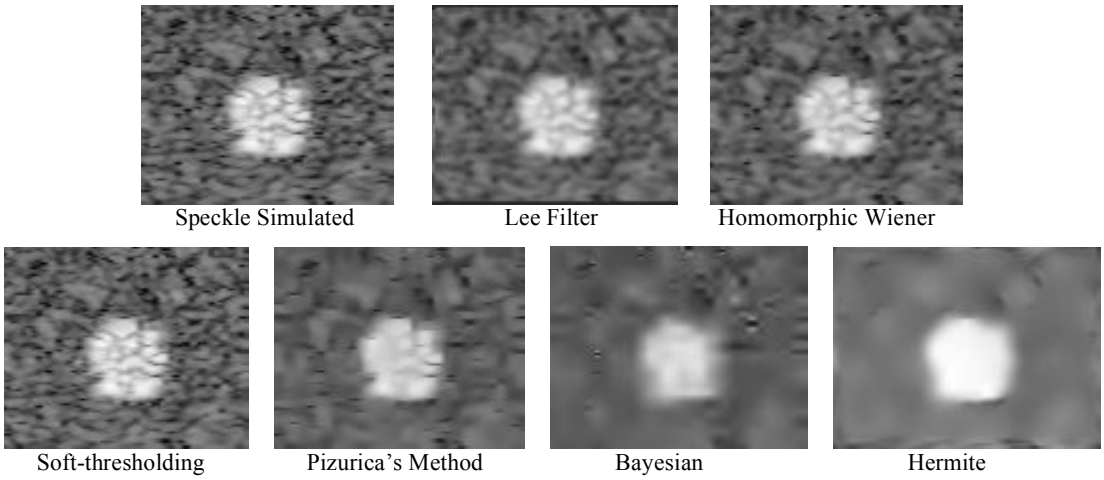

Figure 4. Subjective comparison of different techniques in the image simulated with FIELD II program.

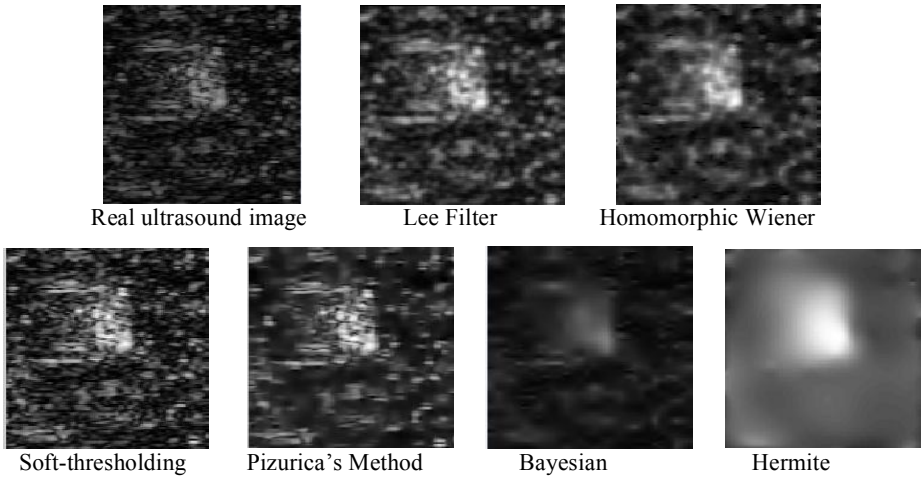

Figure 5. Subjective comparisons of different techniques using a real ultrasound image.

In order to quantify the performance of the used filters, we used three common metrics: Signal to Noise Ratio (SNR), Peak Signal-to-Noise Ratio (PSNR) and the Correlation Coefficient (CoC).

Signal to Noise Ratio. This metric compares the level of the desired signal to the level of background noise.

$$\mathrm{SNR} = 10 \cdot \log_{10}\left(\frac{\sigma_s^2}{\sigma_N^2}\right) \tag{17}$$

where σ_s^2 corresponds to noise free image variance and σ_N^2 represents the error variance between the original image and the reduced speckle image. A large SNR value is associated with a good image quality.

Peak Signal-to-Noise Ratio (PSNR). With this metric the radio between the maximum possible power of a signal and the power of corrupting noise that affects the fidelity of its representation is measured.

$$\mathrm{PSNR} = 10 \cdot \log_{10}\left(\frac{M^2_{\max intensity}}{MSE}\right) \tag{18}$$

Correlation Coefficient (CoC). Measurement that determines the degree in which two variables are associated.

$$\mathrm{CoC} = \left(\frac{\sum (x - \bar{x})(\hat{x} - \bar{x})}{\sqrt{\sum (x - \bar{x})^2 \sum (\hat{x} - \bar{x})^2}}\right) \tag{19}$$

In table 1, we summarize the resulting metrics for the mentioned filtering process. Here, two standard deviations for the speckle pattern are used. From the numerical findings, it can be noticed that the Hermite method presents again the best performance among the filtering algorithms.

Table 1. Calculated parameters.

Evaluated Parameters			
Method	**SNR(dB)**	**PSNR**	**CoC**
$\sigma = 0.4$			
Input Image with speckle noise	7.8231	29.8628	0.9868
Lee Filter	5.0428	22.2583	0.9632
Wiener	8.8585	31.9303	0.9916
Soft-thresholding	8.0444	30.2230	0.9880
Pizurica's method	9.1310	29.8628	0.9839
Bayesian	9.2149	32.6356	0.9930
Hermite	**9.1307**	**40.2814**	**0.9900**
$\sigma = 0.9$			
Input Image with speckle noise	4.2820	22.7811	0.9661
Lee Filter	4.7352	22.9140	0.9457
Wiener	5.8116	25.8389	0.9661
Soft-thresholding	7.4025	30.8080	0.9468
Pizurica's method	7.7186	24.1265	0.9477
Bayesian	7.5756	32.8391	0.9704
Hermite	**8.1459**	**36.9777**	**0.9830**

5.2 Detection results

In the second part of our experiments, we evaluate the performance of the detection task by using the real ultrasound images depicted in the previous section. Findings were evaluated with the Rayleigh-based probability test given by equation (3). For the performance assessment, we used the Receptor Operator Characteristic - ROC curve[3]. This curve evaluates the percentage of false positive rate (sensitivity) vs. true positive rate (specificity).

The ROC curve is compared for the detection process applied onto the original, the filtered images using wavelet-based Bayesian and Hermite-based method. These methods are addressed to elaborate tools that can either replace the human observers or help them in the lesion detection task. In figure 6 the ROC curve for the cases considered is illustrated. As mentioned, the test is carried out with 146 images equally distributed with and without structure (lesion).

The best performance is achieved for the method that presents the ROC curve closest to the vertical axis, so that the largest quantity of true positives and least quantity of false alarms are found. From this figure, it is noted that the best target detection performance is achieved when the images are filtered applying the Hermite transform. Working with speckle images reduces the detection efficiency. The analysis was also made for the Gaussian case taking several random ultrasound images that exhibit Gaussian distributions. We based this method on the fact that the addition of several random variables results in Gaussian distributions. We estimate the corresponding statistic parameters like the covariance matrices from a set of training samples for lesion present and lesion absent cases.

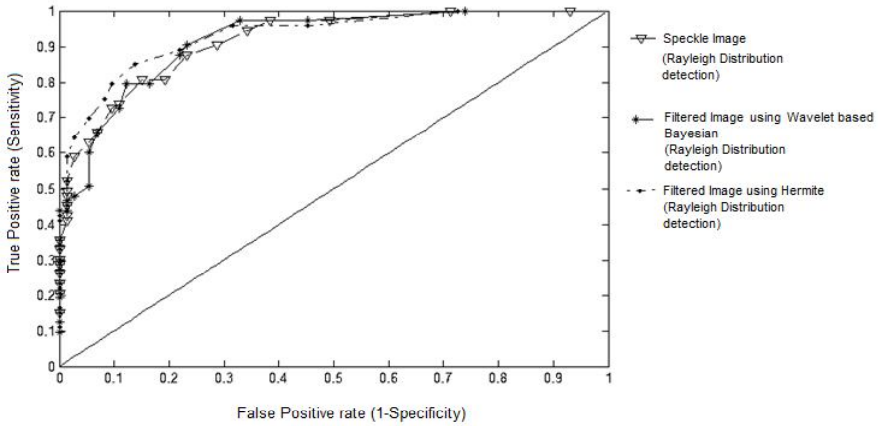

Figure 6. ROC curves of Rayleigh-based observer performance for the original and filtered ultrasound images.

Thresholds for the decision rules are selected manually and experimentally analyzing the set of data. It is worth mentioning that this threshold depends on the characteristics of the samples images. From experimental results, we proved that the distribution of the images does not suffer changes after applying the filtering process. We attribute this result to the fact that filtering techniques reduce speckle but do not eliminate it completely. This allows us employing the studied decision theory for the filtered images as well.

6. CONCLUSIONS

Filtering and detection tasks were analyzed according to signal detection theory in ultrasound images. Filtering techniques visually enhance the appearance of ultrasound images and help in the detection tasks. The best performing system uses a robust multiresolution despeckling method that preserves important features in ultrasound images based on the Hermite transform. It was demonstrated quantitatively and qualitatively that this filter presents the best performance considering the adopted metrics SNR, PSNR and CoC.

On the other hand, we considered two possible observer models for detection tasks of low contrast structures in ultrasound images. Under the assumption of Gaussian and Rayleigh distributions, we adopt the theory of observers for small and low contrast lesion areas. Decision rules are found and the filtering process is included for optimal detection. In this case, it is shown that filtering techniques improve the detectability of the structures. In this contexture aim at designing, we try to design a signal detection and filtering framework for automatic detection task in ultrasound B-scan images. The percentage of detection of lesion increases when the images are previously filtered. In future works, we will analyze different kinds of structures present in ultrasound images and comparisons with the human observer will be included.

ACKNOWLEGEMENT

Authors thank CONACYT México, Universidad Nacional Autónoma de México (UNAM), PAPIIT grant IN113611 and COLCIENCIAS Colombia for the financial support in the project.

REFERENCES

[1] Rousset, P., Gompel, A., Christin-maitre, S., Pugeat, M., Hugol, D., Ghossain, M.A. and Buy, J.N., "Ovarian hyperthecosis on grayscale and color Doppler ultrasound, " Ultrasound. Obstet. Gynecol. 32(5), 694-699 (2008).
[2] Tian, JW., Sun, L.T., Guo, YH., Cheng, H.D. and Zhang, YT., "Computerized-aid diagnosis of breast mass using ultrasound image," Med. Phys. 34, 3158-3164 (2007).
[3] Barrett, HH., Abbey, CK. and E. Clarkson, "Objective assessment of image quality. iii. roc metrics, ideal observers, and likelihood-generating functions," J. Opt. Soc. Am. A. Opt. Image Sci Vis. 15(6), 1520-1535 (1998).
[4] Wu, J. and Chung, A. C. S., "A segmentation model using compound Markov random fields based on a boundary model," IEEE Transaction on Image Processing 16, 241-252 (2007).
[5] Wagner, R. F., Smith, S. W., Sandrik, J. M. and Lopez, H., "Statistics of speckle in ultrasound B-scans," IEEE Transactions on Sonics Ultrasonics 30, 156–163 (1983).

[6] Wagner, R. F., Insana, M. F. and Brown, D. G., "Statistical properties of radio-frequency and envelope-detected signals with applications to medical ultrasound," J. Opt. Soc. Am. A. Opt. Image Sci Vis. 4(5), 910–922 (1987).
[7] Smith, S. W., Wagner, R. F., Sandrik, J. M. and Lopez, H., "Low contrast detectability and contrast/detail analysis in medical ultrasound," IEEE Transactions on Sonics and Ultrasonics 30(3), 164–173 (1983).
[8] Goodman, J. W., "Introduction to Fourier Optics," McGraw-Hill, New York, (1996).
[9] Insana, M. F. and Hall, T. J., "Visual detection efficiency in ultrasonic imaging: A framework for objective assessment of image quality," J. Acoust. Soc. Am. 95(4), 2081-2090 (1994).
[10] Clarkson, E. and Barrett, HH., "Approximations to ideal-observer performance on signal-detection tasks," Applied Optics 39(11), 1783-1793 (2000).
[11] Loizou, C.P., Pattichis, C.S., Pantziaris, M., Istepanian, R.S.H., Pantziaris, M., Tyllis, T., and Nicolaides, A., "Quantitative quality evaluation in ultrasound imaging in carotid artery," Med. Biol. Eng. Comput. 44 (5), 414–426 (2006).
[12] Yu, Y. and Acton, S.T., "Speckle reducing anisotropic diffusion," IEEE Trans. Image Process. 11 (11), 1260–1270 (2002)
[13] Gupta, S., Chauhan, R.C. and Saxena, S.C., "Homomorphic wavelet thresholding technique for denoising medical ultrasound images," Taylor & Francis Int. J. Med. Eng. Technol. 29 (5), 208–214 (2005).
[14] Pižurica, A., Philips, W., Lemahieu and I., Acheroy, M., "A versatile wavelet domain noise filtration technique for medical imaging," IEEE Trans. Medical Imaging 22 (3), (2003).
[15] Yue, Y., Croitoru, M.M., Bidani, A., Zwischenberger, J.B. and Clark, J.W., "Non-linear multiscale wavelet diffusion for speckle suppression and edge enhancement in ultrasound images," IEEE Trans. Medical Imaging 25(3), (2006).
[16] Escalante-Ramírez, Boris. "The Hermite transform as an efficient model for local image analysis: An application to medical image fusion, " Journal Computers and Electrical Engineering 34(2), 99-110 (2008).
[17] Escalante-Ramírez, Boris and López-Caloca, Alejandra A. "The Hermite Transform: An Efficient Tool for Noise Reduction and Image Fusion in Remote Sensing in Signal and Image Processing for Remote Sensing," Taylor and Francis, 537-555 (2006).
[18] Silván-Cárdenas, José L., Escalante-Ramírez, Boris, "The multiscale hermite transform for local orientation analysis," IEEE Transactions on Image Processing 15(5), 1236-1253 (2006).
[19] Achim, A., Bezerianos, A., and Tsakalides, P.," Novel Bayesian multiscale method for speckle removal in medical ultrasound images," IEEE Transactions on Medical Imaging 20(8), 772-783 (2001).
[20] Donoho, D. L., "De-noising by soft-thresholding," IEEE Trans. Inform. Theory 41(3), 613–627 (1995).
[21] Grace Chang, S., "Adaptive Wavelet Thresholding for Image Denoising and Compression," IEEE Trans. Image Processing, 9(9), (2000).
[22] Gupta, S., "Locally adaptive wavelet domain Bayesian processor for denoising medical ultrasound images using Speckle modelling based on Rayleigh distribution," IEE Proc.-Vis. Image Signal Process 152(1), (2005).
[23] Amara Graps, "An introduction to wavelets," IEEE Computational Science and Engineering 2(2), 50 - 61 (1995).
[24] Barba, J., L. and Vargas, Q. L., "Microcalcifications Detection System through Discrete Wavelet Analysis and Image Enhancement Techniques," Proc. 40th Southeastern Symposium on System Theory 40, 118-121 (2008).
[25] Mihçak, M.K. Kozintsev, I., Ramchandran, K. and Moulin, P., "Low complexity image denoising based on statistical modeling of wavelet coefficients," IEEE Signal Process. Lett. 6(12), (1999).
[26] Lee, J.S., "Speckle analysis and smoothing of synthetic aperture radar images," Comput. Graph. Image Process. 17(1), 24-32 (1981).
[27] Burckhardt, C., "Speckle in ultrasound B-mode scans," IEEE Trans. Sonics Ultrason. 25(1), 1-6 (1978).
[28] Papoulis, A., [Probability random variables and stochastic processes] MHL, New York, (1991).
[29] Roger J. Zemp, "Detection Performance Theory for Ultrasound Imaging Systems," IEEE Transactions on Medical Imaging 24 (3), (2005).
[30] Jain A.K., [Fundamental of digital Image Processing], Prentice Hall, Upper Saddle River, (1989).
[31] Jensen, J.A., "Field: A Program for Simulating Ultrasound Systems," Medical & Biological Engineering & Computing 34 (1), 351-353 (1996).
[32] Kalaivani Narayanan, S. and Wahidabanu, R.S.D., "A View on Despeckling in Ultrasound Imaging," International Journal of Signal Processing Image Processing and Pattern Recognition 2 (3), (2009).
[33] Lim, Jae S., [Two-Dimensional Signal and Image Processing], Prentice Hall, Englewood Cliffs, NJ, 548 (1990).
[34] L. Barba, L. Vargas, C. Torres, L. Mattos, "Digital Correlation based on Wavelet Transform for Image Detection," J. Phys.: Conf. Ser. 274(1), (2011).